Transactions of the Materials Research Society of Japan 33[2] 197-203 (2008)

The Role of Solute Al in Hot Deformation of Mg – Al Alloys

N. Srinivasan and P. Rama Rao*
Defence Metallurgical Research Laboratory, Hyderabad, India.
Fax: 0091-40-243-40683, e-mail: nsrinivasandsnr@gmail.com
*International Advanced Research Centre for Powder Metallurgy and New Materials, Hyderabad, India.
Fax:0091-40-277-67593, e-mail: pallerama_rao@yahoo.co.in

Abstract: Magnesium is the eighth most abundant element in the earth's crust and also the third most commonly used structural metal following steel and Al. Several Al alloys used in automobile, aerospace, nuclear and sports industries are being replaced by Mg alloys due to their high specific strength and good damping capacity. The HCP crystal structure with a limited number of operative slip systems render Mg alloys inherently poorly workable. This drawback has restricted use of these alloys mostly in the as-cast condition. Present research endeavours the world-over are therefore mostly aimed at overcoming this drawback so that Mg wrought alloys find wider application. Just as Mg is a commonly used alloying addition to Al, so also Al in Mg alloys. We have used the processing map technique to study the hot deformation behaviour of Mg-Al alloys. The results show that the addition of Al improves workability at high speeds of deformation, which feature has direct implication to Mg-based component manufacture. It is also found that the tailoring of microstructure through thermo-mechanical processing (TMP) can be achieved as the addition of Al provides a variety of safe processing windows.

Keywords: Magnesium, Deformation, Processing map, Flow instability, Workability.

1. INTRODUCTION

Magnesium alloys merit as structural materials owing to their high specific strength, acceptable impact properties and creep resistance, high damping capacity and good machinability. Fine-grained wrought Mg exhibits better yield strength than Al[1] and some of the wrought Mg alloys potentially can be expected to replace steel and other light Al and Ti alloys[2]. However, the utility of Mg alloys is restricted to the as-cast condition due to poor workability associated with their HCP crystal structure with limited number of independent slip systems. Most of the present day research is therefore directed at improving workability through alloying and mechanical processing.

Aluminium is the most commonly used alloying element in Mg[3]. The solubility of Al ranges from 1 at% at 100°C to 11.5 at % (12.7 wt%) at the eutectic temperature (437°C). The alloys in excess of 5 wt% Al can be heat treated. In addition to excellent castability and solid solution strengthening offered by the solute Al, it also reduces the 'c' spacing of HCP Mg[3,4] as well as its stacking fault energy (SFE)[5]. These factors have a direct influence on Mg deformation.

The present authors have investigated hot deformation of Mg-Al binary solid solution alloys. The microstructural evolution during hot deformation is highly sensitive to the process parameters due to the strong dependence of non-basal slip on temperature and strain-rate which is responsible for the varying workability exhibited by the material. There are several studies addressing issues specific to superplastic deformation in the commercial wrought Mg-Al alloys[6-12]. However, there are no detailed studies on microstructural development and its relationship to the effects of solute Al during hot deformation of as-cast Mg alloys. Thus, the aim of the present investigation is to study the role of Al during hot deformation of binary as-cast Mg-Al alloys with 1wt% and 3wt% Al. For this purpose, the processing map technique has been resorted to.

The *processing-map* technique has been widely used to understand the workability of many materials[13] in terms of the various microstructural mechanisms operating at the different deformation conditions. The technique is developed on the basis of dynamic materials modelling (DMM)[14] which considers the complementary relationship between the rate of visco-plastic heat generation induced by deformation and the rate of energy dissipation associated with microstructural mechanisms occurring during deformation. A non-dimensional efficiency index η is used to represent the power dissipation through microstructural mechanisms and is given as

$$\eta = 2m / (m+1) \qquad \text{----(1)}$$

where m is the strain rate sensitivity of the material which is a function of deformation temperature and strain rate. The contour plot of the iso-efficiency η values on the temperature – strain rate field constitutes the processing map. As the dissipation characteristics vary for different microstructural mechanisms, each domain on the map can be correlated to a single dominant mechanism operating under those conditions of the domain and, therefore, the *processing-maps* are known as *power dissipation maps.* In addition to the η contours, the instability criterion given by the equation

$$\xi = \{\partial \ln \{m / (m+1)\} / \partial \ln \dot{\varepsilon}\} + m < 0 \qquad \text{----(2)}$$

is applied to delineate the temperature – strain rate regimes of flow instability on the processing map. A detailed description of the development of the model as

well as the significance of η value in the interpretation of the domains have been given by Prasad et al.[14,15].

2. EXPERIMENTAL

The as-cast binary alloys Mg – 1wt% Al and Mg – 3 wt.% Al were received in the form of cylindrical ingots of 75 mm diameter and 235 mm height. The compression test coupons of aspect ratio 1.5 were prepared by electro-discharge wire cutting and subsequent machining. The tests were conducted on a servo-hydraulic testing machine (DARTEC, UK) with microprocessor control. The compression tests were carried out under isothermal conditions at temperatures and true strain rates ranging from 250 - 550°C and $3x10^{-4} - 10^{2}$ s^{-1} respectively, which encompass the entire hot working range of Mg alloys. The samples were coated with graphite / teflon to reduce friction at the die – workpiece interface and the initial height was reduced to 50% corresponding to a true strain of 0.69. The deformed samples were water-quenched immediately after the test and were cut along the compression axis for metallographic examination. The load – stroke data recorded for each compression test were used to derive the true stress – true plastic strain values which in turn were used to compute the efficiency and the instability parameters as a function of temperature and strain rate. The software PROMOTE (PROcess MOdelling TEchnique) developed for this purpose was used to generate the processing maps.

3. RESULTS AND DISCUSSION

3.1. Processing map

The processing maps of the two binary Mg alloys with 1wt% and 3wt% Al obtained at a strain $\in$=0.5 are shown in Fig.1(a) and (b) respectively. The hatched regions correspond to unstable flow where the instability parameter ξ (Eqn. 2) takes a negative value. It is striking that the region of flow instability in the processing map of Mg 1% Al is much wider and dominates the processing map for this alloy (Fig.1a). On the other hand, the efficiency domains in the stable flow region of Mg-3% Al are more distinct and these are as follows: *domain I* with a peak efficiency (η_p) of about 56% at 450°C / 3 $x10^{-4}$ s^{-1}, *domain II* with a peak efficiency of about 42% at 550°C / 10^{-1} s^{-1}, *domain III* with a peak efficiency of about 42% at 450°C / 10^{2} s^{-1} and *domain IV* with a peak efficiency of about 28% occurring at 250°C / 10^{-1} s^{-1}. A detailed characterization of these domains in terms of the underlying dominant microstructural mechanisms has been reported elsewhere[16]. The *domain I* corresponds to grain boundary sliding (GBS), the *domains II & III* correspond to dynamic recrystallization (DRX) and the *domain – IV* corresponds to dynamic recovery (DRV). The processing map of Mg – 1wt% Al exhibits similar domains corresponding to I, II and IV of Mg-3% Al under stable flow conditions. However, the deformation conditions of the *domain III* of Mg-3%Al correspond to flow instability conditions in Mg-1%Al. The peak efficiency conditions of the stable flow domains of Mg-1% Al are : η_p=36% at 475°C / 3 x 10^{-4} s^{-1} for *domain I*, η_p = 45% at 550°C / 3 x 10^{-2} s^{-1} for *domain II* and η_p = 23% at 250°C / 10^{-1} s^{-1} for *domain IV*. For the sake of comparison, the processing map of pure Mg generated by Sivakesavam et al[17] is presented in Fig.2. The two dominant domains reported for pure Mg are (1) the wedge cracking domain with a maximum efficiency of 60% at 550°C / 10^{-3} s^{-1} and (2) the DRX domain with a peak efficiency of 34% occurring at 425°C / 0.3 s^{-1}. These two domains correspond respectively to *domains I & II* of Mg-Al alloys. However, their peak efficiency conditions of the domains are shifted considerably when compared to those observed in Mg.

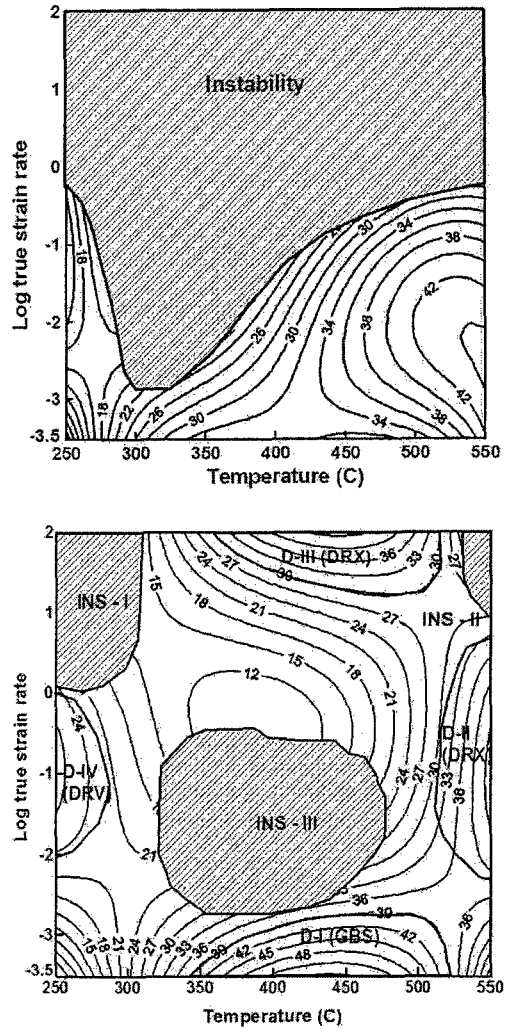

Fig.1 The processing maps of (a) Mg – 1wt%Al and (b) Mg – 3wt%Al alloys. The contour values represent iso-efficiency of power dissipation. The *instability regimes* are hatched.

In the case of Mg – 1% Al, at higher strain rates (>1s^{-1}), the flow instability regime (ξ < 0) occurs at all temperatures and it occurs over an inverted cone region at strain rates less than 1 s^{-1}, having a base ranging from 250 to 400°C and an apex at 325°C (Fig.1a). In contrast, in the case of Mg-3% Al, the flow instability regimes at higher strain rates are restricted to temperatures lower than 300°C (INS - I) and higher than 525°C (INS-II) (Fig.1b). The instability region (INS-III)

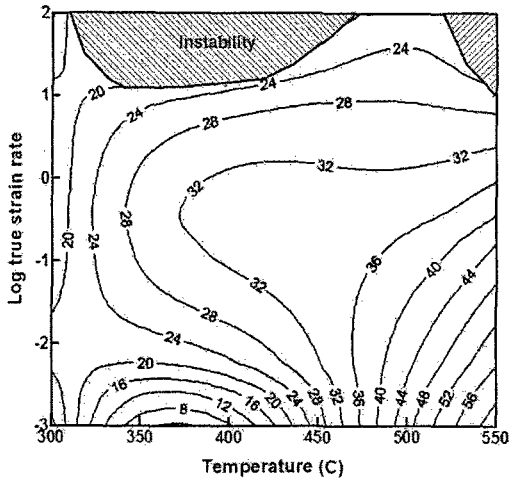

Fig.2 The processing map of pure Mg[17] at the strain 0.5. The contour values represent iso-efficiency of power dissipation. The *instability regimes* are shown as hatched regions.

occurs at the intermediate strain rate range 10^{-3} to10^{-1} s^{-1}, and in the temperature range 350 – 450°C, which is similar to that occurring over an inverted cone region for Mg-1% Al. Although at higher strain rates the flow instability has been reported for pure Mg, the intermediate flow instability regime (INS – III) is absent for pure Mg[17].

In the subsequent sections, the variations observed in the stable flow domains and in the instability regimes of Mg[17], Mg-1%Al & Mg-3%Al (present work) are discussed, and are correlated with the effect of solute Al.

2. STABLE FLOW DOMAINS

2.1 Grain Boundary Sliding (GBS)

The underlying mechanism of *domain I* observed at the lower strain-rates is grain boundary sliding and is present in Mg and in both the Mg – Al alloys. It is more distinct in the case of Mg-3% Al than in the case of Mg-1%Al. The temperature and the strain rate conditions of *domain I* for all three materials are compared in Fig.3. In the case of pure Mg, the domain spreads over wider strain rate range (< 1 s^{-1}) and occurs over the temperature range 475 - 550°C. In the presence of solute Al, the strain rate range of the domain is restricted to lower strain rates (< 10^{-3} s^{-1}) due to the solute drag effect (SD) of Al which is found to be more severe in dilute Mg alloys[18]. However, the optimum strain rate condition for GBS corresponding to peak efficiencies lie at lower strain rates (< 10^{-3} s^{-1}) for all three materials. On the other hand, with increasing Al content, the peak efficiency temperature shifts to lower temperatures from 550°C for pure Mg to 475°C for Mg – 1% Al and to 425°C for Mg – 3%Al. Similarly, the temperature range is also shifted to lower temperatures.

In our earlier investigation on Mg-3%Al[16], the rate controlling mechanism for GBS was seen to be slip accommodated grain boundary diffusion which was also reported in many commercial Mg-Al alloys[7] exhibiting superplasticity. The reduction in 'c' lattice spacing of solid solution HCP Mg with Al addition promotes non-basal slip[4] and, in particular, reduces the activation energy for prismatic slip[3]. Therefore,

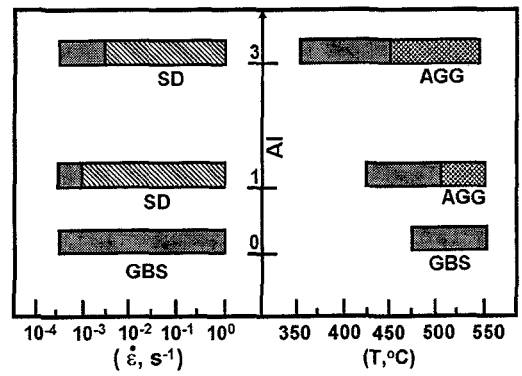

Fig.3 The comparative bar diagram for the processing conditions of GBS domains (*domain I*) of pure Mg and Mg – Al alloys. The conditions of other mechanisms namely, AGG and SD, operating at the neighbourhood of the GBS domain are also indicated.

increasing solute Al facilitates the on-set of slip accommodated GBS at lower temperatures (Fig.3) and shifts the peak efficiency temperature to lower temperatures (Fig.1a&b).

Further, in two different studies on commercial Mg-Al alloys, namely AZ31 & AZ61, by Perez-Predo and Ruano[19,20], it was observed that the abnormally growing grains were oriented with prismatic planes parallel to the sheet plane. As the activation energy for prismatic slip is reduced with Al content[3], the solute concentration is expected to play a significant role in the development of prismatic texture during hot compression and, consequently, in abnormal grain growth (AGG). Inevitably, the onset of AGG, hinders GBS at higher temperatures. This is evident from the processing map of Mg-3%Al (Fig.1b) in which there is a significant decrease in efficiency values beyond 500°C at lower strain rates (< 10^{-3} s^{-1}). In contrast, GBS domain observed for pure Mg exhibits the peak efficiency (60%) at 550°C / 10^{-3} s^{-1} indicating the absence of AGG in pure Mg.

2.2 Dynamic Recrystallization (DRX)

The dominant microstructural mechanism under the conditions of *domains II & III* is interpreted to be DRX[16]. The temperature – strain rate ranges of the *domains II* and III are shown in Figs. 4(a) and (b) respectively. The *domain III* is present only for Mg-3%Al while the *domain II* is exhibited by both the materials. Further, the rate controlling mechanisms have been shown to be stress assisted cross slip and thermally activated climb in *domains II & III* respectively[16]. Although the peak efficiency of the *domain II* occurs at 550°C for both the materials, the strain-rate condition corresponding to peak efficiency is increased by more than an order of magnitude for Mg – 3% Al (10^{-1} s^{-1}) compared to that for Mg – 1% Al ($3x10^{-3}$ s^{-1}) (Fig.1). A similar DRX domain was observed for pure Mg at 425°C / 0.3s^{-1} (Fig.2). In pure Mg, the maximum temperature for the domain is limited to 450°C since at higher temperatures (> 450°C) GBS becomes the dominant mechanism. On the other hand, even though GBS is favoured only at much lower strain rates in Mg-Al alloys, the solute drag (SD) phenomenon and solid solution strengthening impede the DRX process

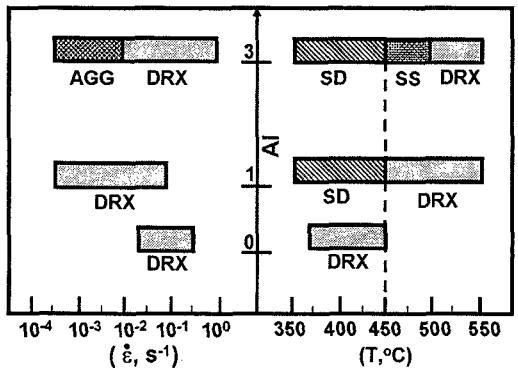

Fig.4(a) The comparative bar diagram for the processing conditions of DRX domains (*domain II*) of pure Mg and Mg – Al alloys. The conditions of other mechanisms namely, AGG and SD, operating at the neighbourhood of the GBS domain are also indicated.

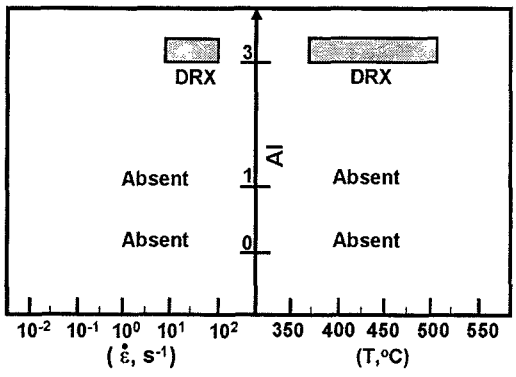

Fig.4(b) The comparative bar diagram for the processing conditions of DRX domains (*domain III*) of pure Mg and Mg – Al alloys.

restricting the range of the *domain II* to the region of higher temperatures. The marginally wider temperature range (450 - 550°C) for Mg – 1% Al than for Mg – 3%Al (500 - 550°C) may be attributed to the higher degree of solid solution strengthening (SS) in the latter material. Moreover, the AGG at higher temperatures and lower strain rates is more pronounced in Mg – 3%Al and restricts the domain to higher strain rates. This results in lower peak efficiency in Mg-3% Al (42%) compared to that in Mg-1%Al (46%).

The DRX domain (III) is observed only in the processing map of Mg-3%Al, with a peak efficiency of 42% at 450°C/10^2 s^{-1} (Fig.4b). The flow stress – strain response as a function of strain rate for the two Mg-Al alloys recorded during hot compression at 450°C is shown in Figs.5(a) & (b), where (a) and (b) correspond to Mg alloys with 1% and 3% Al respectively. Mg-3%Al exhibits higher flow stress values due to enhanced solid solution strengthening and markedly higher at higher strain rates. Despite the high flow stress values, the curves display stable flow behaviour with initial work-hardening followed by mild flow softening due to the occurrence of DRX. On the other hand, anomalous flow behaviour is observed for Mg-1%Al at a strain rate of 10^2 s^{-1}. In this case, initial rapid work-hardening is followed by severe flow softening on reaching the peak flow stress. Such anomalous features are associated with

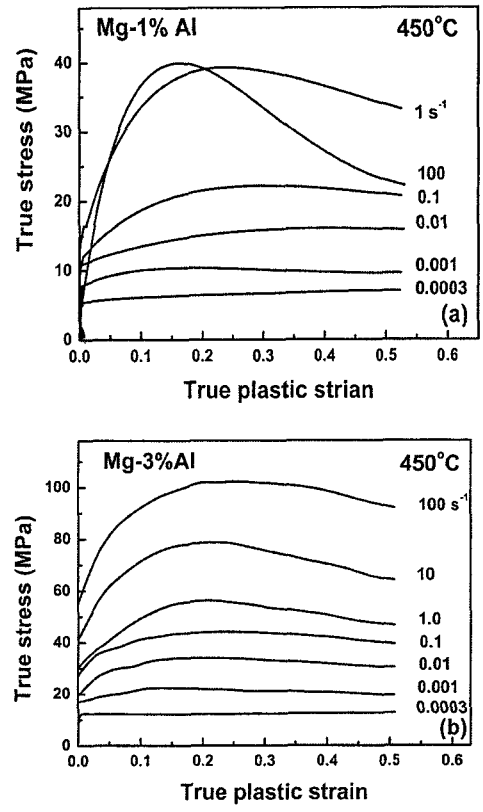

Fig.5 True stress – true plastic strain plots for (a) Mg – 1%Al and (b) Mg – 3%Al alloys obtained at 450°C for various true strain rates.

flow localization (shear bands) commonly observed at high rates of deformation[13]. Although solid solution strengthening in Mg-1% Al is expected to be less compared to that in Mg-3%Al, the rapid initial work-hardening observed in the former alloy suggests that non-basal slip is not effective in providing homogeneous deformation. This, in turn, results in flow instability. In Mg-3%Al, the non-basal slip becomes operational due to higher Al content for reasons discussed in the earlier section and promotes DRX. The absence of a distinct high strain rate DRX domain for pure Mg can be explained as due to lack of ability to generate sufficient dislocation density required for DRX.

2.3 Dynamic Recovery (DRV)

Fig.6 compares the deformation conditions of DRV process. The *domain IV* (DRV) occurs below 300°C in the strain rate range from 10^{-2} to 10^{0} s^{-1} in the processing map of Mg – 3%Al. The microstructural evidences and linear relationship of inverse flow stress with work hardening rate presented in our earlier investigations[16] support that DRV is the dominant microstructural mechanism in *domain IV*. The DRV domain of Mg-1%Al is confined to temperatures below 275°C. At these low temperatures (< 300°C) the basal glide is dominant[18]. The respective stress-strain response of Mg-1% Al & Mg – 3% Al alloys at 250°C and at various strain-rate conditions are shown in Fig 7(a) & (b). The flow curves corresponding to peak efficiency in DRV domains (250°C / 10^{-1} s^{-1}) exhibit steady state flow

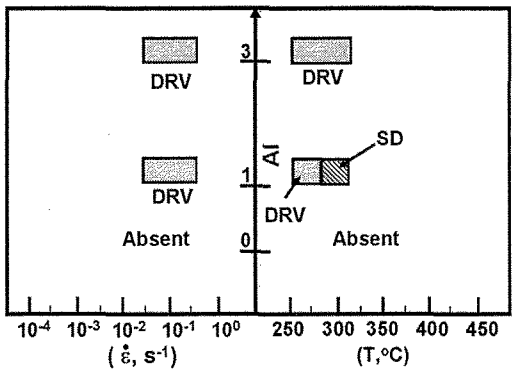

Fig.6 The comparative bar diagram for the processing conditions of DRV domains (*domain IV*) of pure Mg and Mg – Al alloys.

after initial work hardening, which is reported to be the characteristic flow behaviour under DRV conditions for several materials[21]. Further, the absence of DRV domain for pure Mg in the investigated temperature and strain rate is attributable to non-availability of solid solution strengthening. In contrast, solid solution strengthening (SS) and easy basal slip due to reduction in lattice spacing contribute to the occurrence of DRV in Mg – Al alloys. These effects of Al on DRV domain are further supported by the observation that the DRV domain is restricted to lower range of temperatures (< 275°C) in Mg – 1% Al compared to that in Mg 3% Al (< 300°C).

3. Flow instability

Figs.8(a) & (b) summarize the deformation conditions of flow instabilities associated with localized shear and solute drag. All three materials exhibit localized shear (shear band) at high strain rates. Understandably, only the Mg – Al alloys exhibit flow instability associated with solute drag. In Mg - 1%Al, the flow instability regime at higher strain rates extends up to $1s^{-1}$ and spreads over the entire temperature range of investigation. In Mg – 3%Al, the high strain rate flow instability occurs on either side of DRX domain (III) (350-500°C). The regime extends up to 1 s^{-1} below 350°C and is confined to strain rates higher than 10 s^{-1} above 500°C. In similarity to Mg – 1% Al, in pure Mg the flow instability regime occurs over the entire temperature range excepting over a small range from 450 to 500°C where stable flow is observed. However, it is restricted to higher strain rates (>10 s^{-1}) compared to that in Mg – 1% Al (> $1s^{-1}$). In the lower temperature range, the larger strain rate spread (up to $1s^{-1}$) in Mg – Al alloys compared to pure Mg could be due to enhanced solid strengthening in Al containing Mg alloys. The significant reduction in lattice spacing with increasing Al content makes the non-basal slip increasingly operative at higher temperatures and, consequently, the flow instability is restricted to higher strain rates (> 10 s^{-1}) as seen in the processing map of Mg – 3%Al. Also, in the case of Mg – 3% Al, at the intermediate temperature range (350 – 500°C), the rate of critical dislocation density produced and the rate kinetics of DRX, with thermally activated climb process as the rate controlling mechanism, may be in such equilibrium that stable flow

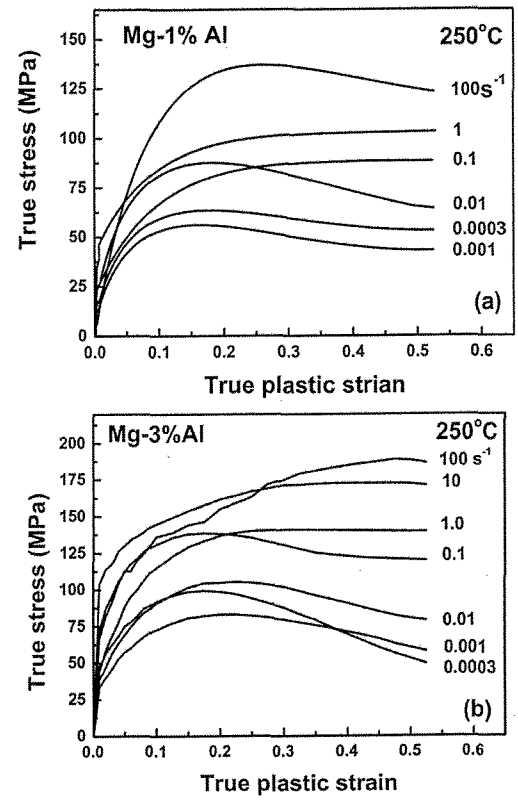

Fig.7 True stress – true plastic strain plots for (a) Mg – 1%Al and (b) Mg – 3%Al alloys obtained at 250ºC for various true strain rates.

is promoted. The corresponding flow curve obtained at 450°C / $100s^{-1}$ for Mg – 3% Al (Fig. 5b) exhibits initial mild work hardening up to a critical strain followed by gradual softening. On the other hand, the anomalous flow softening exhibited by the flow curve obtained at 450°C / 100 s^{-1} for Mg – 1%Al (Fig. 5a) corroborates the view that homogenous deformation is hampered due to flow localization.

In the strain rate range below 1 s^{-1}, flow instability is attributed to solute drag in Mg – Al alloys. Also, it was reported that in Al containing Mg alloys, the solute atmosphere around the dislocations retard climb and

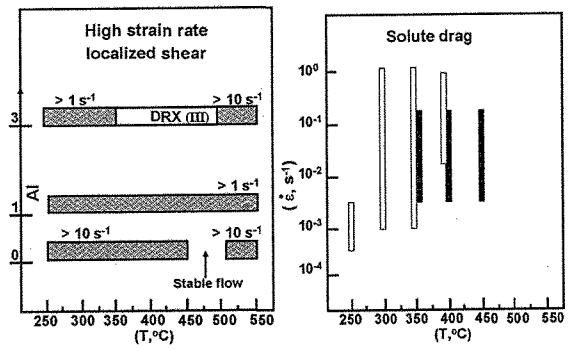

Fig.8 The comparative bar diagrams for the processing conditions of *flow instability regimes* of pure Mg and Mg – Al alloys, associated with (a) high strain rate localized shear and (b) solute drag (unfilled bars and filled bars correspond to Mg-1wt%Al and Mg-3wt%Al respectively).

glide which in turn affects dynamic restoration processes (DRX & DRV)[18] impairing the workability of the material[13]. Solute drag effect is more severe in dilute alloys[18] and the same has been observed in Mg – 1%Al (Fig.1a). Vagarali and Langdon[22] reported solute drag in Mg - 0.8% Al. They found the binding energy between the solute atom and the dislocation to be 20kJ mol^{-1}. The anomalous flow behaviour leading to negative strain rate sensitivity observed at low strain rates for Mg – 1% Al (Fig.7a) in the present investigation further supports this argument. Although no such flow anomaly is recorded for Mg - 3%Al, the rise in flow stress observed in the instability regime when plotted as a function of temperature was attributed to solute drag[16].

4. HOT WORKABILITY

The central purpose of evaluating hot deformation using the processing map technique is to predict hot workability of the investigated materials. From the above discussion, it is evident that the binary alloy Mg – 3% Al possesses better hot workability compared to Mg – 1% Al. In general, deformation conditions of dynamic restoration processes (DRX & DRV) have been reported to improve the hot workability in several materials[23]. The processing maps exhibit distinct domains for DRX and DRV processes and the deformation conditions corresponding to peak efficiencies are considered to be the optimum conditions for the underlying mechanisms of the respective domains. For that reason, the hot workability associated with such domains of Mg-3%Al were validated. The variation of hot tensile ductility measured at the nominal strain rate of 10^{-1} s^{-1} and the corresponding efficiency (η) variation are plotted as a function of temperature in Fig.9. The strain rate was so chosen that the temperature variation spans DRV domain (IV) at lower temperatures (< 300°C), flow instability regime in the intermediate temperature range (300 – 475°C) and DRX domain (II) at higher temperatures (> 475°C). Both ductility and efficiency exhibit similar variations with temperature. They show a minimum in the flow instability regime and an increase in the lower as well as the higher temperature regimes as they approach DRV and DRX domains respectively. Also, the ductility under DRX condition is more than that under DRV condition suggesting that DRX domain provides better processing window for good workability for the material. Therefore, the corresponding DRX deformation condition (T > 500°C, 10^{-2} < $\dot{\varepsilon}$ < 10^{0} S^{-1}) can be exploited for cast ingot break-down process (cogging process). In addition to this DRX domain (II), Mg – 3%Al exhibits another DRX domain (III) which is absent in Mg-1%Al. The unique DRX domain of Mg-3%Al offers a processing window at high rates of deformation (> 10 s^{-1}). Such high strain rates are encountered in metal working processes such as hammer forging, extrusion and rolling. To validate the DRX domain (III), the material (Mg- 3%Al) with an initial grain size of about 250μm (Fig.10a) was extruded under *domain III* conditions which resulted in fine grain structure (18μm) (Fig.10b) in the extruded rod. The grain refinement obtained corroborates the occurrence of DRX when

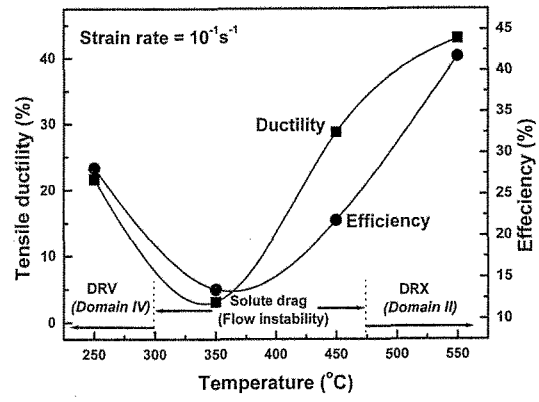

Fig.9 The variations of tensile ductility and efficiency as a function of temperature at a nominal strain rate 10^{-1} s^{-1} of Mg – 3%Al alloy.

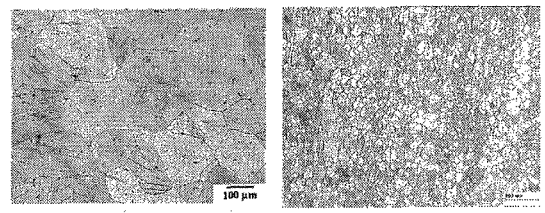

Fig.10 (a) The initial microstructure of the as – cast Mg – 3%Al alloy and (b) the fine grain microstructure obtained on extrusion at the high strain rate DRX condition (*domain III*).

Mg – 3%Al is processed at intermediate temperatures (350 - 500°C) and higher strain rates (> 10 s^{-1}).

5. CONCLUSIONS

Processing map technique was used to demarcate the deformation conditions for stable and unstable flow in binary Mg – Al alloys with 1 wt% and 3 wt% solute Al . The alloy Mg – 3% Al exhibits wider stable flow region compared to Mg – 1% Al. The effect of solute Al content on the various mechanisms underlying DRX, DRV and GBS domains have been discussed in terms of the corresponding deformation conditions. Even though the processing maps of both the materials show similar domains below 1 s^{-1}, Mg – 3%Al exhibits a unique high strain rate DRX domain above 10 s^{-1} over the temperature range from 350 to 500°C marking it a significant result of the present work. The flow instability observed below 1 s^{-1} in Mg – Al alloys was due to solute drag. It is a significant observation from the present work that in the Mg-1%Al alloy, the phenomenon of solute drag results in flow instability. The production of fine equiaxed microstructure with significant reduction in grain size in hot extruded Mg-3%Al validates the unique DRX *domain III* observed in the present work. Furthermore, the present studies of hot deformation of Mg-1%Al and Mg-3%Al alloys help us to understand why commercial alloys containing 3wt% Al, namely AZ30 and AZ31, have come to be so popularly used.

Acknowledgements

The authors are thankful to the Director, DMRL, Hyderabad for supporting the activity and giving permission to publish it. The high temperature testing facilities extended to this investigation by Materials Behaviour Group (MBG) and Rolling Technology group (RTG) of DMRL are acknowledged. One of the authors (NS) is indebted to Prof. Y.V.R.K. Prasad for introducing him to the *processing map technique,* and thanks him for valuable suggestions during the investigation. One of the authors (PRR) gratefully acknowledges the financial support of Dept. Sci. and Technol. (DST), Govt. of India and Japan Society for Promotion of Science (JSPS) which enabled a presentation to have made based on this paper at the 17th IKETANI Conf. and the Doyama symposium on Advanced Materials held in Tokyo in September, 2007. PRR is also grateful to the Indian Space Research Organization (ISRO) for the award of a Professorship to him.

References

1. H. Watarai, Science and Technology Trends, Quarterly review no. 18, (2006) 84 - 97.
2. T. Mukai, M. Yamanoi, H. Watanabe and K. Higashi, Scripta Materialia, 45 (2001) 89 – 94.
3. Magnesium Technology, Eds. H.E. Friedrich, B.L. Mordike, Springer – Verlag, Berlin, Heidelberg, Germany, 2006.
4. Z. Drozd, Z. Trojanová and S. Kúdela, J. alloys and compounds, 378 (2004) 192 – 195.
5. H. Somekawa, K. Hirai, H. Watanabe, Y. Takigawa and K. Higashi : Mater. Sci. Engg., A, 407 (2005) 53-61.
6. Xin Wu and Yi Liu: Scripta Materialia, 46 (2002) 269 – 274.
7. H. Watanabe, T.Mukai, M.Mabuchi and K.Higashi; Acta Mater. 49 (2001) 2027-2037.
8. W.J. Kim, S.W. Chung , C.S. Chung and D. Kum ; Acta Mater. 49 (2001) 3337-3345.
9. J.C.Tan and M.J.Tan; Mat. Sci. Engg. A 339 (2003) 81-89.
10. C.J.Lee and J.C.Huang; Acta Mater. 52 (2004) 3111-3122.
11. T.Mukai, H. Tsutsui, H.Watanabe, K.Ishikiwa, Y. Okanada, M. kohzu, S.Tanabe and K. Higashi: Key Engg. Materials, 171-174 (2000) 337-342.
12. H. Watanabe, T. Mukai, M. Kohazu, S.Tanabe and K. Higashi: Acta Mater. 47 (1999) 3753.
13. Y.V.R.K. Prasad and S.Sasidhara: Hot Working guide: A compendium on processing maps, ASM, International, Metals Park, OH (1997).
14. Y.V.R.K. Prasad, H.L. Gegel, S.M. Doraivelu, J.C. Malas, J.T. Morgan, K.A. Lark, D.R. Barker: Metall. Trans. 15 A (1984) 1883-1892.
15. Y.V.R.K. Prasad: Indian J. Technol., 28 (1990) 435-451.
16. N. Srinivasan, Y.V.R.K. Prasad and P. Rama Rao, Mat. Sci. Engg. A, 476 (2008) 149.
17. O. Sivakesavam, I.S.Rao and Y.V.R.K. Pradad: Mat. Sci. Technol., 9 (1993) 805-810.
18. A. Mwembela, E.B. Konopleva and H.J. Mc Queen: Scr. Materialia, 37 (1997) 1789-1795.
19. M.T. Pérez – Prado and O.A. Ruano, Scripta Materialia, 46 (2002) 149 – 155.
20. M.T. Pérez – Prado and O.A. Ruano, Scripta Materialia, 48 (2003) 59 – 64.
21. Thermodynamic Processing of Metallic Materials, Pregamon Materials Series, ed. R.W. Cahn, Vol. 11, 2007.
22. S.S. Vagarali and T.G. Langdon, Acta Metall., 30 (1982) 1157-1170.
23. W.J. McG. Tegart, Acta Metall., 9 (1961) 614-617.

(Recieved April 5, 2008 ; Accepted April 21,2008)